Available online at www.sciencedirect.com
SCIENCE DIRECT®
ELSEVIER
Journal of Sound and Vibration 290 (2006) 968–990
JOURNAL OF SOUND AND VIBRATION
www.elsevier.com/locate/jsvi

Moving least square Ritz method for vibration analysis of plates

L. Zhou*, W.X. Zheng

School of Quantitative Methods and Mathematical Sciences, University of Western Sydney, Locked Bag 1797, Penrith South DC, NSW 1797, Australia

Received 16 August 2004; received in revised form 11 April 2005; accepted 2 May 2005
Available online 25 July 2005

Abstract

This paper presents a novel numerical method, the moving least square Ritz method (MLS-Ritz), for free vibration analysis of classical thin plates. The proposed method utilizes the strength of the moving least square approach to define the Ritz trial function for the transverse displacement of the plates. A set of points is pre-selected on the calculation domain of a plate that forms the basis for the MLS-Ritz trial function. The edge support conditions of the plate are satisfied by forcing the boundary points to meet the geometric boundary conditions of the plate via a point substitution technique. Virtual points (points outside the plate domain) are introduced for clamped edges to improve the convergence and accuracy of the calculations. Square and right-angled isosceles triangular plates of various combinations of edge support conditions are selected to examine the validity and accuracy of the MLS-Ritz method. Extensive convergence studies are carried out to investigate the influence of the MLS mesh size, the MLS support radius, the number of Gaussian integration points and the shape of the MLS weight function on the proposed method. Comparing with the existing Ritz methods, the MLS-Ritz method is highly stable and accurate and is extremely flexible for dealing with plates of arbitrary shapes and boundary conditions.

*Corresponding author. Tel.: +61 2 47360 456; fax: +61 2 47360 867.
E-mail address: l.zhou@uws.edu.au (L. Zhou).

0022-460X/$ - see front matter
doi:10.1016/j.jsv.2005.05.004

1. Introduction

Plate structures are one of the most important types of structures used in civil, mechanical, marine and aerospace engineering. Vibration of plates has been studied extensively since 1787 [1–6] due to its importance in the design of plate structures and many of the important studies in this field were documented in Leissa's monograph [2] and a series of reviews [7–12].

Various analytical and numerical methods have been developed to investigate the vibration behaviour of plates, ranging from the superposition method [13–15], Levy approach [6,16,17], point collocation method [18], finite difference method [19], differential quadrature (DQ) method [20], Ritz method [5], meshless method [21] to the finite strip method and the finite element (FE) method [22,23]. Although analytical methods are important to give an insightful understanding of the vibration behaviour and to provide benchmark frequencies of plates, numerical methods are preferred in the vibration analysis of plates due to the fact that most of the plate vibration problems do not admit analytical solutions. While the FE method is still the dominant numerical method in this field, many alternative methods such as the finite strip method, Ritz method and DQ method are developed to improve the efficiency and accuracy of vibration analysis of plates. Cheung [22] proposed the finite strip method for plate analysis which is proven to be highly efficient to deal with plates of regular shapes. The p-Ritz method developed by Liew and his associates [5] in the past decade has made a significant impact on the vibration analysis of plates and shells. Their approach was able to enforce the geometric boundary conditions of plates automatically and to deal with plates of various shapes and different internal line supports. The DQ method proposed by Bellman et al. [24] starts to make its impact in the area of plate analysis and a large number of publications can be found in the open literature [20,25]. Recently, the discrete singular convolution (DSC) method developed by Wei and his associates [26] showed great potential in the analysis of plates, especially in the high frequency analysis of plates [27].

The moving least square (MLS) technique was originally used for data fitting [21]. In recent years, researchers have applied the MLS technique in the analysis of solid mechanics problems by developing the meshless method or element free Garlerkin method [21]. The MLS technique is employed to establish the shape functions in the numerical analysis process. The MLS technique was also applied in conjunction with the DQ approach to analyse the bending and buckling of plates [28] and electromagnetic field problems [29].

This paper presents a new numerical method, called the MLS-Ritz method, for the vibration analysis of plates. The classical thin plate (Kirchhoff plate) theory is employed in this study. The MLS data interpolation technique is utilized to establish the Ritz trial function for the transverse displacement of a plate. The geometric boundary conditions of the plate are enforced through a point substitution technique. Extensive convergence and comparison studies are carried out for square and right-angled isosceles plates of various support conditions to verify the correctness and accuracy of the proposed numerical method.

2. Mathematical modelling

Fig. 1 shows a rectangular plate of length a, width b and uniform thickness h in a Cartesian coordinate system. The plate is of the modulus of elasticity E, the Possion ratio υ and the mass

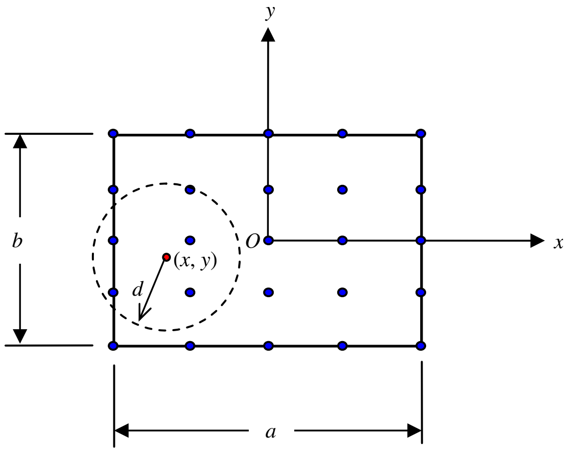

Fig. 1. Dimensions and coordinate system for a rectangular plate.

density ρ. The Lagrangian of the plate based on the classical plate theory in harmonic vibration can be expressed as [2]

$$F = \frac{D}{2}\int_A \left\{ \left(\frac{\partial^2 w}{\partial x^2} + \frac{\partial^2 w}{\partial y^2} \right)^2 - 2(1-\upsilon)\left[\frac{\partial^2 w}{\partial x^2}\frac{\partial^2 w}{\partial y^2} - \left(\frac{\partial^2 w}{\partial x \partial y} \right)^2 \right] \right\} \mathrm{d}A - \frac{1}{2}\rho h \omega^2 \int_A w^2 \, \mathrm{d}A, \tag{1}$$

where $w(x, y)$ is the transverse displacement at the midsurface the plate, $D = Eh^3/[12(1-\upsilon^2)]$ is the flexural rigidity of the plate, A is the area of the plate and ω is the circular frequency of the vibration which needs to be determined.

The Ritz method is employed in this study. The Ritz trial function is first established through the MLS technique [21]. A number of pre-determined points are selected on the calculation domain of the plate (see Fig. 1). The distribution of the points can be regular or irregular, depending on the requirement of the problem at hand. For convenience and simplicity, uniformly distributed grid points are used in this study.

The transverse displacement at an arbitrary point (x, y) (see Fig. 1) on the plate domain can be approximately evaluated as

$$w^h(x, y) = \sum_{i=1}^{m} p_i(x, y) a_i = \mathbf{p}^{\mathrm{T}}(x, y)\mathbf{a}, \tag{2}$$

in which $w^h(x, y)$ is the approximate value of $w(x, y)$, m is the number of basis functions that form a complete space, $\mathbf{p}(x, y) = [p_1(x, y) \;\; p_2(x, y) \;\; \cdots \;\; p_m(x, y)]^{\mathrm{T}}$ is a finite set of basis functions of a complete space, and $\mathbf{a} = [a_1 \;\; a_2 \;\; \cdots \;\; a_m]^{\mathrm{T}}$ is the unknown coefficients, respectively.

Applying the MLS technique, we can determine the unknown coefficients $\mathbf{a}$ by minimizing the following weighted quadratic form

$$\Pi(\mathbf{a}) = \sum_{i=1}^{n} g_i(r)(w^h(x_i, y_i) - w_i)^2 = \sum_{i=1}^{n} g_i(r)(\mathbf{p}^{\mathrm{T}}(x_i, y_i)\mathbf{a} - w_i)^2, \tag{3}$$

where (x_i, y_i), $i = 1, 2, \ldots, n$, are the n grid points in the neighbourhood of the point (x, y), w_i is the nominal displacement at point (x_i, y_i), and $g_i(r)$ is the weight function used in the MLS fitting which can take different forms as shown in Ref. [21]. We propose the following weight function to be used in this study

$$g_i(r) = \begin{cases} (1 - r^2)^k & \text{if } r \leqslant d, \\ 0 & \text{if } r > d, \end{cases} \tag{4}$$

in which $r = \sqrt{(x - x_i)^2 + (y - y_i)^2}/d$ is the normalized distance between the point (x, y) and the ith grid point (x_i, y_i), d is the radius of support (see Fig. 1) and k is an integer which can be adjusted to optimize the MLS fitting.

Minimizing Eq. (3) with respect to the unknown coefficients $\mathbf{a}$, we can obtain the unknown coefficients as follows:

$$\mathbf{a} = \mathbf{A}^{-1}\mathbf{B}\mathbf{w}, \tag{5}$$

where

$$\mathbf{A} = \sum_{i=1}^{n} g_i(r)\mathbf{p}(x_i, y_i)\mathbf{p}^{\mathrm{T}}(x_i, y_i), \tag{6}$$

$$\mathbf{B} = \begin{bmatrix} g_1(r)\mathbf{p}(x_1, y_1) & g_2(r)\mathbf{p}(x_2, y_2) & \cdots & g_n(r)\mathbf{p}(x_n, y_n) \end{bmatrix}, \tag{7}$$

$$\mathbf{w} = [w_1 \;\; w_2 \;\; \cdots \;\; w_n]^{\mathrm{T}}. \tag{8}$$

Substituting Eq. (5) into Eq. (2), the Ritz trial function for the transverse displacement $w(x, y)$ can be approximated in terms of the nominal displacement values of the grid points within the radius of support d as

$$w(x, y) = w^h(x, y) = \sum_{i=1}^{n} R_i(x, y)w_i = \mathbf{R}\mathbf{w} = \mathbf{w}^T\mathbf{R}^T, \tag{9}$$

$$\mathbf{R} = [R_1(x, y) \;\; R_2(x, y) \;\; \cdots \;\; R_i(x, y) \;\; \cdots \;\; R_n(x, y)], \tag{10}$$

$$R_i(x, y) = \mathbf{p}^T(x, y)\mathbf{A}^{-1}g_i(r)\mathbf{p}(x_i, y_i). \tag{11}$$

We may also express the Ritz trial function in terms of the nominal displacement values of all grid points in the calculation domain as

$$w(x, y) = w^h(x, y) = \sum_{i=1}^{N} R_i(x, y)w_i = \mathbf{R}\mathbf{w} = \mathbf{w}^{\mathrm{T}}\mathbf{R}^{\mathrm{T}}, \tag{12}$$

where N is the total number of grid points in the calculation domain. $R_i(x, y)$ may be evaluated using Eq. (11) if the ith grid point (x_i, y_i) is within the radius of support d of point (x, y), or $R_i(x, y) = 0$ otherwise.

The first and second derivatives of the Ritz trial function [Eq. (12)] with respect to x and y can be expressed as

$$\frac{\partial w(x,y)}{\partial x} = \frac{\partial w^h(x,y)}{\partial x} = \sum_{i=1}^{N} \frac{\partial R_i(x,y)}{\partial x} w_i = \mathbf{R}_x \mathbf{w} = \mathbf{w}^{\mathrm{T}} \mathbf{R}_x^{\mathrm{T}}, \tag{13}$$

$$\frac{\partial w(x,y)}{\partial y} = \frac{\partial w^h(x,y)}{\partial y} = \sum_{i=1}^{N} \frac{\partial R_i(x,y)}{\partial y} w_i = \mathbf{R}_y \mathbf{w} = \mathbf{w}^{\mathrm{T}} \mathbf{R}_y^{\mathrm{T}}, \tag{14}$$

$$\frac{\partial^2 w(x,y)}{\partial x^2} = \frac{\partial^2 w^h(x,y)}{\partial x^2} = \sum_{i=1}^{N} \frac{\partial^2 R_i(x,y)}{\partial x^2} w_i = \mathbf{R}_{xx} \mathbf{w} = \mathbf{w}^{\mathrm{T}} \mathbf{R}_{xx}^{\mathrm{T}}, \tag{15}$$

$$\frac{\partial^2 w(x,y)}{\partial y^2} = \frac{\partial^2 w^h(x,y)}{\partial y^2} = \sum_{i=1}^{N} \frac{\partial^2 R_i(x,y)}{\partial y^2} w_i = \mathbf{R}_{yy} \mathbf{w} = \mathbf{w}^{\mathrm{T}} \mathbf{R}_{yy}^{\mathrm{T}}, \tag{16}$$

$$\frac{\partial^2 w(x,y)}{\partial xy} = \frac{\partial^2 w^h(x,y)}{\partial xy} = \sum_{i=1}^{N} \frac{\partial^2 R_i(x,y)}{\partial xy} w_i = \mathbf{R}_{xy} \mathbf{w} = \mathbf{w}^{\mathrm{T}} \mathbf{R}_{xy}^{\mathrm{T}}. \tag{17}$$

Substituting Eqs. (12)–(17) into Eq. (1), the total potential energy functional can be expressed as follows

$$F = \tfrac{1}{2}\mathbf{w}^{\mathrm{T}}\left(\mathbf{K} - \omega^2 \mathbf{M}\right)\mathbf{w}, \tag{18}$$

where the stiffness matrix $\mathbf{K}$ and the mass matrix $\mathbf{M}$ have the dimension of $N \times N$ and are given respectively by

$$\mathbf{K} = D \int_A \left[\mathbf{R}_{xx}^{\mathrm{T}} \mathbf{R}_{xx} + \mathbf{R}_{yy}^{\mathrm{T}} \mathbf{R}_{yy} + \upsilon \mathbf{R}_{xx}^{\mathrm{T}} \mathbf{R}_{yy} + \upsilon \mathbf{R}_{yy}^{\mathrm{T}} \mathbf{R}_{xx} + 2(1-\upsilon) \mathbf{R}_{xy}^{T} \mathbf{R}_{xy}\right] \mathrm{d}A, \tag{19}$$

$$\mathbf{M} = \rho h \int_A \mathbf{R}^{\mathrm{T}} \mathbf{R} \, \mathrm{d}A. \tag{20}$$

A point substitution approach is proposed in this paper in conjunction with the MLS interpolation scheme to impose the geometric boundary conditions of the plate. Fig. 2 shows a typical rectangular plate with free, simply supported and clamped edges. A set of pre-selected uniform grid points are assigned on the calculation domain. Grid points are located on the plate boundaries, inner domain as well as outer domain (virtual points) for clamped edges. Note that the number of grid points on the outer domain is equal to the number of grid points on the clamped edges as shown in Fig. 2.

We can group the nominal displacements on the grid points of the plate into two categories $\mathbf{w}_B$ and $\mathbf{w}_I$, i.e.

$$\mathbf{w} = \begin{bmatrix} \mathbf{w}_B \\ \mathbf{w}_I \end{bmatrix}, \tag{21}$$

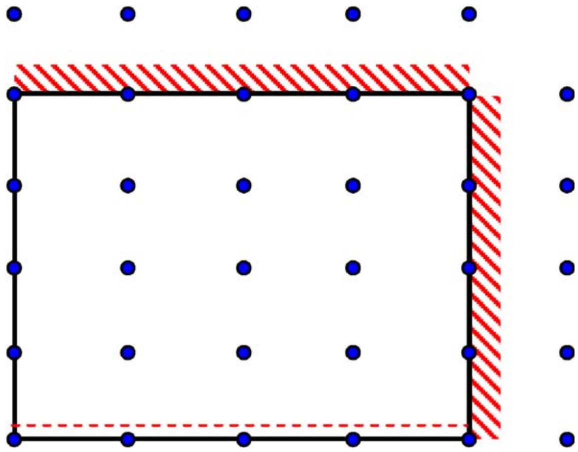

Fig. 2. MLS grid point arrangement for a rectangular plate with free, simply supported and clamped edges.

where $\mathbf{w}_B$ contains all nominal displacements of the points on the simply supported and clamped edges and on the outer domain, and $\mathbf{w}_I$ contains all nominal displacements of the points on the free edge/s and the inner domain, respectively. In view of Eqs. (12)–(14), the geometric boundary condition for a grid point (x_j, y_j) on a simply supported edge is given by

$$w(x_j, y_j) = w^h(x_j, y_j) = \sum_{i=1}^{N} R_i(x_j, y_j) w_i = 0. \tag{22}$$

And if the point is on a clamped edge, the geometric boundary conditions are

$$w(x_j, y_j) = w^h(x_j, y_j) = \sum_{i=1}^{N} R_i(x_j, y_j) w_i = 0, \tag{23}$$

$$\frac{\partial w(x_j, y_j)}{\partial s} = \frac{\partial w^h(x_j, y_j)}{\partial s} = \sum_{i=1}^{N} \frac{\partial R_i(x_j, y_j)}{\partial s} w_i = 0, \tag{24}$$

where s denotes the normal direction to the clamped edge/s. Applying boundary conditions for all grid points on the simply supported and clamped edges, we can obtain a linear equation system given by

$$\begin{bmatrix} \mathbf{Q} & \mathbf{S} \end{bmatrix} \begin{bmatrix} \mathbf{w}_B \\ \mathbf{w}_I \end{bmatrix} = \mathbf{0}. \tag{25}$$

The nominal displacements of the grid points on the simply supported and clamped edges and on the outer domain can be expressed as

$$\mathbf{w}_B = -\mathbf{Q}^{-1} \mathbf{S} \mathbf{w}_I. \tag{26}$$

The nominal displacements for all grid points can then be expressed in terms of $\mathbf{w}_I$ as follows:

$$\mathbf{w} = \begin{bmatrix} \mathbf{w}_B \\ \mathbf{w}_I \end{bmatrix} = \begin{bmatrix} -\mathbf{Q}^{-1}\mathbf{S} \\ \mathbf{I} \end{bmatrix} \mathbf{w}_I = \mathbf{T}\mathbf{w}_I. \tag{27}$$

Note that the geometric boundary conditions of the plate are effectively enforced by applying the above point substitution approach.

Substituting Eq. (27) into Eq. (18), the total potential energy functional can be expressed as

$$F = \frac{1}{2}\mathbf{w}_I^{\mathrm{T}}\left(\overline{\mathbf{K}} - \omega^2\overline{\mathbf{M}}\right)\mathbf{w}_I, \tag{28}$$

where

$$\overline{\mathbf{K}} = \mathbf{T}^{\mathrm{T}}\mathbf{K}\mathbf{T}, \tag{29}$$

$$\overline{\mathbf{M}} = \mathbf{T}^{\mathrm{T}}\mathbf{M}\mathbf{T}. \tag{30}$$

Minimizing the Lagrangian (Eq. (1)) with respect to $\mathbf{w}_I$, we have

$$\left(\overline{\mathbf{K}} - \omega^2\overline{\mathbf{M}}\right)\mathbf{w}_I = \mathbf{0}. \tag{31}$$

The vibration frequency ω can be determined by solving the generalized eigenvalue equation defined by Eq. (31).

3. Results and discussions

The proposed MLS-Ritz method is examined in this section for its validity and accuracy. The natural frequencies of several selected square and right-angled isosceles triangular plates are obtained. The Poisson ratio υ is set to be 0.3 and the non-dimensional frequency parameter is defined as $\lambda = (\omega a^2/\pi^2)\sqrt{\rho h/D}$, where a is the length of the plates.

Convergence studies must be carried out to verify the validity of the MLS-Ritz method. There are several parameters that can vary in the proposed method. Firstly, the basis function used in Eq. (2) can be any finite basis function of a complete space. We propose to use the 2-D complete polynomial as the basis function in this study. If the degree P of the polynomial is zero, $\mathbf{p}(x,y) = 1$. If $P = 2$, $\mathbf{p}(x,y) = [1 \;\; x \;\; y \;\; x^2 \;\; xy \;\; y^2]^{\mathrm{T}}$. Integration needs to be carried out for Eqs. (19) and (20) over the plate domain. The influence of the integer number k in the weight function (Eq. (4)) on the accuracy of the method will be examined. Finally, the number of MLS grid points and the effective range of the radius of support d need to be evaluated. The accuracy of the MLS-Ritz method is verified against the known benchmark results.

3.1. Square plates

For a square plate, the plate domain is divided into four equal segments (see Fig. 3) and the Gaussian quadrature is employed to evaluate Eqs. (19) and (20). The number of sufficient Gaussian points will be determined for carrying out the integration.

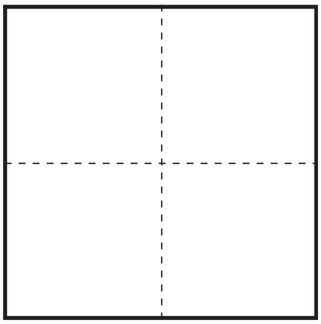

Fig. 3. Four equal segments used in Gaussian quadrature.

Table 1
Variation of frequency parameters λ versus the value of P for a simply supported square plate with $k = 10$, $d = 0.5a$, 20×20 Gaussian points and 15×15 MLS grid points

P	Mode sequence					
	1	2	3	4	5	6
0	2.0001	5.0002	5.0002	8.0002	10.0057	10.0059
1	2.0000	5.0000	5.0000	8.0001	10.0007	10.0007
2	2.0000	5.0001	5.0001	8.0000	10.0003	10.0003
3	2.0000	5.0000	5.0000	8.0000	10.0001	10.0001
4	2.0000	5.0000	5.0000	8.0000	10.0000	10.0000
5	2.0000	5.0000	5.0000	8.0000	10.0000	10.0000
6	2.0000	5.0000	5.0000	8.0000	9.9999	9.9999

A simply supported square plate is first considered in the convergence study. To study the influence of the degree P of the 2-D complete polynomial basis function $\mathbf{p}(x, y)$, the number of Gaussian points in each segment is set to be 20×20, the value of k in the weight function is fixed at 10, a set of 15×15 MLS grid points is used and the radius of support d is equal to $0.5a$, where a is the length of the square plate. Table 1 shows the variation of the first six frequency parameters for the simply supported square plate as the degree P of the 2-D polynomial changes from 0 to 6. We observe that the frequency parameters in general decrease as the degree P of the polynomial basis function increases. Good convergence is achieved even with $P = 2$. The frequency parameters of the 5th and 6th modes with $P = 6$ are 9.9999 which is slightly lower than the exact value of 10. It may be caused by numerical roundoff error in the calculation. We also noted that the computational time of the MLS-Ritz method is increased rapidly when the degree P of the 2-D polynomial basis function increases. This is because the number of terms used in the approximation of $w(x, y)$ in Eq. (2) increases significantly as P increases.

Table 2 shows the same convergence study for a clamped square plate. It is observed that for the first four vibration modes, the frequency parameters converge well as the degree of the 2-D polynomial basis function $P = 1$. Further increase in the value of P, we observe that the frequency parameters for the 4th–6th modes oscillate slightly. In general, $P = 2$ is sufficient to provide converged results.

Table 2
Variation of frequency parameters λ versus the value of P for a clamped square plate with $k = 10$, $d = 0.5a$, 20×20 Gaussian points and 15×15 MLS grid points

P	Mode sequence					
	1	2	3	4	5	6
0	3.6461	7.4377	7.4377	10.9704	13.3322	13.3964
1	3.6461	7.4364	7.4364	10.9648	13.3320	13.3952
2	3.6461	7.4364	7.4364	10.9647	13.3323	13.3955
3	3.6461	7.4364	7.4364	10.9646	13.3320	13.3952
4	3.6461	7.4364	7.4364	10.9648	13.3320	13.3953
5	3.6461	7.4363	7.4363	10.9645	13.3319	13.3950
6	3.6461	7.4363	7.4363	10.9646	13.3319	13.3950

Table 3
Convergence of frequency parameters λ against the MLS grid point size for a simply supported square plate with $P = 2$, $k = 10$, $d = 0.5a$ and 20×20 Gaussian points

MLS grid points	Mode sequence					
	1	2	3	4	5	6
5×5	6061	53051	55369	72450	226535	3715952
7×7	2.0210	5.2818	5.2818	8.2356	11.0872	11.0916
9×9	2.0019	5.0357	5.0357	8.0330	10.2036	10.2039
11×11	2.0000	5.0012	5.0012	8.0022	10.0041	10.0044
13×13	2.0000	5.0001	5.0001	8.0000	10.0005	10.0006
15×15	2.0000	5.0001	5.0001	8.0000	10.0003	10.0003
17×17	2.0000	5.0000	5.0000	8.0000	10.0002	10.0002
19×19	2.0000	5.0000	5.0000	8.0000	10.0000	10.0000

Tables 3 and 4 examine the variation of the frequency parameters of a simply supported square plate and a clamped square plate with respect to the MLS grid point size. While the MLS grid point size varies from 5×5 to 19×19, the values of $P = 2$, $k = 10$ and $d = 0.5a$ and 20×20 Gaussian points are employed in the calculation. The frequency parameters for both simply supported and clamped square plates decrease monotonically as the MLS grid point size increases. Excellent convergence is achieved for all cases in Tables 3 and 4 when the MLS grid point size reaches 15×15 and more.

The number of Gaussian points required for generating accurate results by the MLS-Ritz method is examined. Tables 5 and 6 show the convergence pattern of the frequency parameters for a simply supported square plate and a clamped square plate against the Gaussian points used in each of the four segments in the plate domain, respectively. The values of $k = 10$, $d = 0.5a$ and $P = 2$ and 15×15 MLS grid points are used in the computation. We observe that the number of Gaussian points affects the frequency parameters significantly. When the number of Gaussian points is small ($\leqslant 5 \times 5$), the frequency parameters are erroneous due to the poor accuracy of the

Table 4
Convergence of frequency parameters λ against the MLS grid point size for a clamped square plate with $P = 2$, $k = 10$, $d = 0.5a$ and 20×20 Gaussian points

MLS grid points	Mode sequence					
	1	2	3	4	5	6
5×5	8.4900	20.2614	20.2631	28.5606	39.0445	40.8206
7×7	2.4228	5.8519	5.8519	8.8486	12.0883	12.0965
9×9	3.6521	7.4610	7.4610	11.0214	13.4037	13.4589
11×11	3.6472	7.4394	7.4442	10.9827	12.3181	13.3415
13×13	3.6461	7.4366	7.4366	10.9651	13.3331	13.3963
15×15	3.6461	7.4364	7.4364	10.9647	13.3323	13.3955
17×17	3.6461	7.4364	7.4364	10.9647	13.3320	13.3953
19×19	3.6461	7.4364	7.4364	10.9647	13.3320	13.3952

Table 5
Variation of frequency parameters λ versus the number of Gaussian points for a simply supported square plate with $k = 10$, $d = 0.5a$, $P = 2$ and 15×15 MLS grid points

Gaussian points	Mode sequence					
	1	2	3	4	5	6
3×3	2.29E-06	2.82E-06	5.42E-06	6.14E-06	1.82E-05	5.54E-05
4×4	0.4928	0.4928	2.2243	2.5920	4.1820	4.3016
5×5	1.4577	4.1372	4.1372	5.5687	6.0195	7.8331
6×6	1.9294	4.9583	4.9583	7.9836	8.1130	8.5060
7×7	1.9997	4.9983	4.9983	7.9978	10.0104	10.0106
8×8	2.0000	5.0008	5.0008	8.0009	9.9948	9.9949
9×9	2.0000	4.9996	4.9996	7.9996	10.0012	10.0012
10×10	2.0000	5.0003	5.0003	8.0003	10.0005	10.0005
11×11	2.0000	4.9999	4.9999	7.9999	10.0000	10.0000
12×12	2.0000	5.0001	5.0001	8.0001	10.0004	10.0004
13×13	2.0000	5.0000	5.0000	8.0000	10.0002	10.0002
14×14	2.0000	5.0001	5.0001	8.0000	10.0003	10.0003
15×15	2.0000	5.0001	5.0001	8.0000	10.0002	10.0003
16×16	2.0000	5.0001	5.0001	8.0000	10.0003	10.0003
17×17	2.0000	5.0001	5.0001	8.0000	10.0002	10.0003
18×18	2.0000	5.0001	5.0001	8.0000	10.0003	10.0003
19×19	2.0000	5.0001	5.0001	8.0000	10.0003	10.0003
20×20	2.0000	5.0001	5.0001	8.0000	10.0003	10.0003

Gaussian integration. The frequency parameters oscillate around the converged values as the number of Gaussian points increases from 6×6 to 13×13 for the simply supported square plate and to 14×14 for the clamped square plate, respectively. The frequency parameters are stabilized when the number of Gaussian points increases further. We observe that 20×20 Gaussian points for each integration segment are sufficient to provide accurate integration results used in the

Table 6
Variation of frequency parameters λ versus the number of Gaussian points for a clamped square plate with $k = 10$, $d = 0.5a$, $P = 2$ and 15×15 MLS grid points

Gaussian points	Mode sequence					
	1	2	3	4	5	6
3×3	1.15E-05	3.32E-05	6.05E-05	1.06E-04	1.60E-04	6.90E-04
4×4	3.57E-04	0.9962	1.5027	1.8746	1.8746	3.6918
5×5	2.4289	4.0241	4.0241	4.9972	5.4150	8.5491
6×6	3.4082	6.3377	6.3377	7.5575	8.2131	10.4485
7×7	3.6368	10.8536	12.8746	12.8984	16.5637	16.5637
8×8	3.6453	7.4312	7.4312	10.9609	13.1737	13.2361
9×9	3.6462	7.4374	7.4374	10.9656	13.3282	13.3917
10×10	3.6460	7.4360	7.4360	10.9645	13.3334	13.3965
11×11	3.6461	7.4365	7.4365	10.9647	13.3316	13.3949
12×12	3.6461	7.4364	7.4364	10.9648	13.3327	13.3959
13×13	3.6461	7.4364	7.4364	10.9647	13.3320	13.3953
14×14	3.6461	7.4364	7.4364	10.9647	13.3324	13.3957
15×15	3.6461	7.4364	7.4364	10.9647	13.3322	13.3955
16×16	3.6461	7.4364	7.4364	10.9647	13.3323	13.3955
17×17	3.6461	7.4364	7.4364	10.9647	13.3323	13.3955
18×18	3.6461	7.4364	7.4364	10.9647	13.3323	13.3955
19×19	3.6461	7.4364	7.4364	10.9647	13.3323	13.3955
20×20	3.6461	7.4364	7.4364	10.9647	13.3323	13.3955

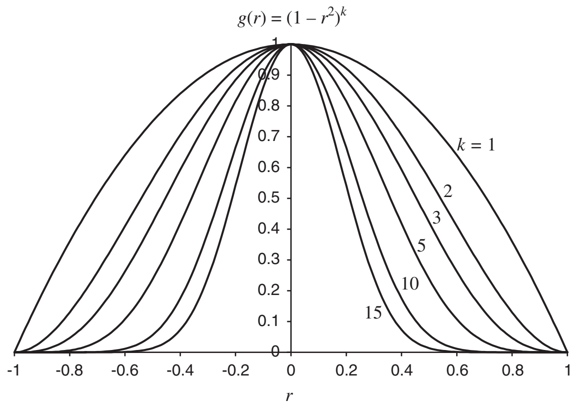

Fig. 4. Influence of the value of k on the MLS weight function.

MLS-Ritz method for square plates. Obviously, increasing the number of Gaussian points will increase the computational time in applying the MLS-Ritz method.

The effect of the values of the integer k on the weight function is depicted in Fig. 4. It is evident that as the value of k increases, the weighted influence in the MLS technique is more concentrated around the region near the fitting point (x, y). The influence of k on the accuracy of the proposed MLS-Ritz method is examined next.

Table 7
Variation of frequency parameters λ versus the value of k for a simply supported square plate with $P = 2$, $d = 0.5a$, 20×20 Gaussian points and 15×15 MLS grid points

k	Mode sequence					
	1	2	3	4	5	6
1	1.9651	3.6612	3.6612	6.2601	8.7269	9.2295
2	2.0007	5.0823	5.0823	8.0110	10.5244	10.5500
3	2.0000	5.0190	5.0190	8.0259	10.0840	10.0863
4	2.0000	5.0024	5.0024	8.0081	10.0360	10.0390
5	2.0001	5.0001	5.0001	8.0004	10.0115	10.0149
6	2.0000	5.0006	5.0006	8.0010	10.0016	10.0019
7	2.0000	5.0002	5.0002	8.0003	10.0039	10.0039
8	2.0000	5.0001	5.0001	8.0001	10.0022	10.0024
9	2.0000	5.0000	5.0000	8.0001	10.0006	10.0006
10	2.0000	5.0001	5.0001	8.0000	10.0003	10.0003
11	2.0000	5.0000	5.0000	8.0000	10.0005	10.0005
12	2.0000	5.0000	5.0000	8.0000	10.0002	10.0002
13	2.0000	5.0000	5.0000	8.0000	10.0000	10.0001
14	2.0000	5.0000	5.0000	8.0000	10.0001	10.0001
15	2.0000	5.0000	5.0000	8.0000	10.0001	10.0001

Table 8
Variation of frequency parameters λ versus the value of k for a clamped square plate with $P = 2$, $d = 0.5a$, 20×20 Gaussian points and 15×15 MLS grid points

k	Mode sequence					
	1	2	3	4	5	6
1	2.2356	5.0639	5.0709	11.2470	12.4406	13.3426
2	3.6642	7.6104	7.6104	11.6907	13.9390	14.5062
3	3.6537	7.4710	7.4710	11.0069	13.3785	13.5265
4	3.6473	7.4399	7.4399	10.9701	13.3673	13.4210
5	3.6460	7.4366	7.4366	10.9658	13.3323	13.3974
6	3.6461	7.4366	7.4366	10.9656	13.3326	13.3958
7	3.6461	7.4367	7.4367	10.9650	13.3326	13.3956
8	3.6461	7.4364	7.4364	10.9649	13.3325	13.3960
9	3.6461	7.4366	7.4366	10.9649	13.3321	13.3952
10	3.6461	7.4364	7.4364	10.9647	13.3323	13.3955
11	3.6461	7.4365	7.4365	10.9647	13.3321	13.3954
12	3.6461	7.4364	7.4364	10.9647	13.3321	13.3953
13	3.6461	7.4364	7.4364	10.9647	13.3322	13.3954
14	3.6461	7.4364	7.4364	10.9647	13.3320	13.3952
15	3.6461	7.4364	7.4364	10.9647	13.3320	13.3952

Tables 7 and 8 present the variation of frequency parameters of a simply supported square plate and a clamped square plate against various values of k in the weight function, respectively. The values of $P = 2$ and $d = 0.5a$, 20×20 Gaussian points and 15×15 MLS grid points are used in

Table 9
Convergence of frequency parameters λ against the radius of support d for a simply supported square plate with $P = 2$, $k = 10$, 20×20 Gaussian points and 15×15 MLS grid points

d/a	Mode sequence					
	1	2	3	4	5	6
0.10	46.7975	52.6090	57.7458	61.4896	66.4244	66.8645
0.15	2.0361	5.3068	5.3922	8.8112	10.0185	10.3138
0.20	2.0062	5.2359	5.2359	8.2434	11.0888	11.0921
0.25	2.0008	5.0144	5.0144	8.0113	10.0787	10.0787
0.30	2.0002	5.0040	5.0040	8.0039	10.0254	10.0254
0.35	2.0000	5.0003	5.0003	8.0006	10.0020	10.0020
0.40	2.0000	5.0000	5.0000	8.0000	10.0003	10.0003
0.45	2.0000	5.0000	5.0000	8.0000	10.0003	10.0003
0.50	2.0000	5.0001	5.0001	8.0000	10.0003	10.0003
0.55	2.0000	5.0000	5.0000	8.0000	10.0009	10.0009
0.60	2.0000	5.0001	5.0001	8.0000	10.0012	10.0012
0.65	2.0000	5.0001	5.0001	8.0001	10.0002	10.0002
0.70	2.0000	5.0000	5.0000	8.0000	10.0008	10.0009
0.75	2.0000	5.0001	5.0001	8.0000	10.0024	10.0026
0.80	2.0000	5.0002	5.0002	8.0003	10.0028	10.0028

Table 10
Convergence of frequency parameters λ against the radius of support d for a clamped square plate with $P = 2$, $k = 10$, 20×20 Gaussian points and 15×15 MLS grid points

d/a	Mode sequence					
	1	2	3	4	5	6
0.10	66.6556	69.0685	72.2822	74.5936	76.1212	76.7361
0.15	3.3912	7.7505	7.7505	11.9050	13.6467	13.7143
0.20	3.8333	8.3798	8.3798	12.1331	16.5325	16.6119
0.25	3.6476	7.4403	7.4403	10.9734	13.3398	13.4029
0.30	3.6470	7.4398	7.4398	10.9736	13.3423	13.4048
0.35	3.6462	7.4372	7.4372	10.9675	13.3338	13.3969
0.40	3.6461	7.4366	7.4366	10.9650	13.3327	13.3959
0.45	3.6461	7.4365	7.4365	10.9648	13.3323	13.3956
0.50	3.6461	7.4364	7.4364	10.9647	13.3323	13.3955
0.55	3.6461	7.4364	7.4364	10.9648	13.3320	13.3954
0.60	3.6461	7.4364	7.4364	10.9648	13.3320	13.3952
0.65	3.6461	7.4364	7.4364	10.9648	13.3322	13.3955
0.70	3.6461	7.4364	7.4364	10.9647	13.3320	13.3952
0.75	3.6461	10.9649	13.3319	13.3951	21.3356	21.3356
0.80	3.6461	10.9646	13.3322	13.3953	21.3310	21.3310

this calculation. We observe that when $k = 1$, the frequency parameters are poorly converged. Further increasing the values of k, frequency parameters oscillate about the converged values for both the simply support and the clamped square plates, respectively. In general, the MLS-Ritz

Table 11
Comparison study of frequency parameters λ for square plates with $P = 2$, $k = 10$, $d = 0.5a$, 20×20 Gaussian points and 15×15 MLS grid points

Cases	Sources	Mode sequence					
		1	2	3	4	5	6
SSSS	Present	2.0000	5.0001	5.0001	8.0000	10.0003	10.0003
	Ref. [3]	2.00000	5.00000	5.00000	8.00000	10.0000	10.0000
CCCC	Present	3.6461	7.4364	7.4364	10.9647	13.3323	13.3955
	Ref. [3]	3.6468	7.4383	7.4383	10.970	13.338	13.399
SCSC	Present	2.9333	5.5466	7.0243	9.5835	10.3568	13.0804
	Ref. [3]	2.93334	5.54664	7.02429	9.58349	10.35667	13.08011
SFSF	Present	0.9759	1.6348	3.7211	3.9460	4.7356	7.1675
	Ref. [3]	0.97586	1.63480	3.72108	3.94595	4.73560	7.16747
SSFS	Present	1.1839	2.8123	4.1741	5.9846	6.2679	9.1488
	Ref. [3]	1.18389	2.81230	4.17410	5.98459	6.26779	9.14871

method can generate accurate frequency parameters when $k \geqslant 10$ and the increase of the k values has a negligible impact on the computational efficiency of the MLS-Ritz method.

The radius of support d of the MLS scheme also plays an important role in obtaining accurate MLS-Ritz results. Tables 9 and 10 show the influence of the radius of support d on the frequency parameters of a simply supported square plate and a clamped square plate, respectively. We use $P = 2$, $k = 10$, 20×20 Gaussian points and 15×15 MLS grid points in this calculation. While a small radius of support d gives erroneous frequency parameters, a very large d value may lead to missing modes as shown in the case for clamped square plate. The optimal range of the radius of support is between $0.4a$ and $6a$ in the considered cases. It is noted that increasing the radius of support d will increase the computational time of the MLS-Ritz method as more neighbourhood grid points are involved in the MLS fitting process.

The accuracy of the MLS-Ritz method can be verified against available benchmark solutions [3] in the open literature. Table 11 presents the frequency parameters for square plates of various boundary conditions obtained by applying the MLS-Ritz method and by Leissa [3]. A four-letter symbol is used to denote the boundary conditions of a square plate. For example, an SFCS plate has a simply supported left edge, a free bottom edge, a clamped right edge and a simply supported top edge, respectively. The MLS-Ritz results are based on $P = 2$, $k = 10$, $d = 0.5a$, 20×20 Gaussian points and 15×15 MLS grid points on the boundaries and inner domain of the plate, respectively. We observe that the MLS-Ritz results are in excellent agreement with the exact solutions for SSSS, SCSC, SFSF and SSFS plates in Ref. [3] and the approximate results for the CCCC plate [3]. The comparison study confirms the high accuracy that the MLS-Ritz method can achieve.

3.2. Right-angled isosceles triangular plates

The validity and accuracy of the MLS-Ritz method is further examined through the vibration analysis of several selected right-angled isosceles triangular plates. The MLS grid points are

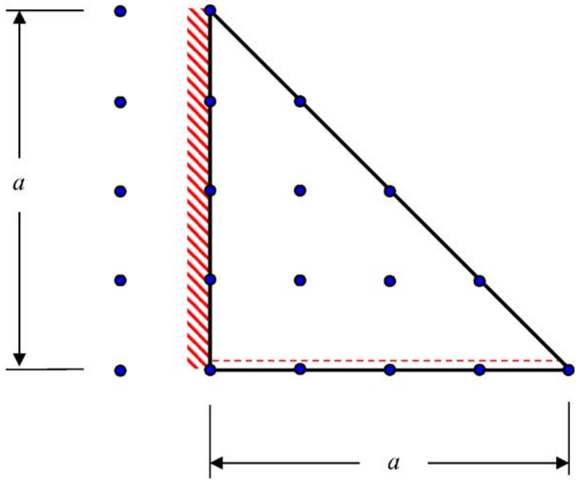

Fig. 5. Distribution of a 5×5 MLS grid points in the analysis.

Table 12
Variation of frequency parameters λ versus the value of P for a simply supported right-angled isosceles triangular plate with $k = 15$, $d = 0.5a$, $N_g = 40$ and 21×21 MLS grid points

P	Mode sequence					
	1	2	3	4	5	6
0	5.0001	10.0009	13.0006	17.0015	20.0039	25.0032
1	5.0000	10.0002	13.0003	17.0011	20.0015	25.0020
2	5.0000	10.0001	13.0001	17.0007	20.0009	25.0010
3	5.0000	10.0000	13.0002	17.0002	20.0004	25.0009
4	5.0000	10.0000	13.0000	17.0001	20.0003	25.0004
5	5.0000	10.0013	13.0013	17.0069	20.0089	25.0031
6	9.8935	10.6089	11.6528	14.4665	20.5306	26.2683

uniformly distributed over the triangular plate domain. For example, Fig. 5 shows the distribution of a 5×5 MLS grid points for a CSF plate where C denotes the clamped left edge, S the simply supported bottom edge and F the free inclining edge, respectively. The notation 5×5 denotes that there are five MLS grid points on the left edge and five on the bottom edge of the plate, respectively. Note that virtual points (points outside the plate domain) are used to enforce the clamped boundary conditions on the left edge of the plate.

The Gaussian quadrature is carried out on the triangular plate domain with the following scheme to determine the number of Gaussian points used in the integration. First, we select the largest dimension in the x direction on the plate domain (in this case, the length of the bottom edge of the plate) and determine the number of Gaussian points N_g to be used. Then, we draw vertical lines through the x coordinates of the N_g Gaussian points. The number of

Table 13
Variation of frequency parameters λ versus the value of P for a clamped right-angled isosceles triangular plate with $k = 10$, $d = 0.5a$, $N_g = 40$ and 21×21 MLS grid points

P	Mode sequence					
	1	2	3	4	5	6
0	9.5028	15.9869	19.7336	24.5995	28.1337	34.0195
1	9.5028	15.9871	19.7338	24.6002	28.1339	34.0199
2	9.5028	15.9870	19.7338	24.6000	28.1335	34.0198
3	9.5028	15.9871	19.7338	24.6004	28.1339	34.0198
4	9.5028	15.9871	19.7338	24.6003	28.1339	34.0198
5	9.5028	15.9871	19.7338	24.6004	28.1339	34.0198
6	9.5028	15.9871	19.7337	24.6003	28.1339	34.0196

Table 14
Convergence of frequency parameters λ against the MLS grid point size for a simply supported right-angled isosceles triangular plate with $P = 3$, $k = 15$, $d = 0.5a$ and $N_g = 40$

MLS grid points	Mode sequence					
	1	2	3	4	5	6
7×7	373.588	621.292	1609.54	2563.54	3180.45	10716.08
9×9	5.4746	11.4446	13.9286	20.2321	22.8061	26.6804
11×11	5.0019	10.0306	13.0224	17.2357	20.2247	25.1559
13×13	5.0002	10.0015	13.0014	17.0090	20.0138	25.0094
15×15	5.0000	10.0002	13.0002	17.0008	20.0016	25.0009
17×17	5.0000	10.0000	13.0002	17.0002	20.0004	25.0009
19×19	5.0000	10.0000	13.0000	17.0001	20.0001	25.0002
21×21	5.0000	10.0000	13.0002	17.0002	20.0004	25.0009
23×23	5.0000	10.0000	13.0000	17.0000	20.0000	25.0000

Gaussian points used on a vertical line is determined by the ratio between the length of the vertical line in the triangular plate domain and the largest x dimension of the triangular plate. We found that when $N_g = 40$, the Gaussian quadrature provides accurate integration results used in the MLS-Ritz method for the vibration analysis of right-angled isosceles triangular plates.

Tables 12 and 13 show the influence of the degree of the 2-D polynomial basis function P on the frequency parameters of a simply supported triangular plate and a clamped triangular plate, respectively. The values of $k = 15$, $d = 0.5a$, $N_g = 40$ and 21×21 MLS grid points are used in the calculation. It is observed that for the clamped plate the increase of the value of P shows no significant impact on the frequency parameters. However, for the simply supported plate, the best range of the P values is between 2 and 4. To strike a balance of efficiency and accuracy, we choose to use $P = 3$ for all subsequent calculations.

Table 15
Convergence of frequency parameters λ against the MLS grid point size for a clamped right-angled isosceles triangular plate with $P = 3$, $k = 15$, $d = 0.5a$ and $N_g = 40$

MLS grid points	Mode sequence					
	1	2	3	4	5	6
7×7	27.738	48.150	65.409	82.227	125.007	179.536
9×9	9.6517	16.6063	20.1005	26.0896	29.4062	35.2701
11×11	9.5064	15.9888	19.7410	24.5306	28.1291	34.0533
13×13	9.5031	15.9868	19.7348	24.5985	28.1289	34.0203
15×15	9.5029	15.9870	19.7342	24.5998	28.1352	34.0217
17×17	9.5028	15.9871	19.7338	24.6002	28.1341	34.0192
19×19	9.5028	15.9871	19.7337	24.6003	28.1339	34.0196
21×21	9.5028	15.9871	19.7338	24.6004	28.1339	34.0198
23×23	9.5028	15.9871	19.7338	24.6004	28.1339	34.0199

Table 16
Variation of frequency parameters λ versus the value of k for a clamped right-angled isosceles triangular plate with $P = 3$, $d = 0.5a$, $N_g = 40$ and 21×21 MLS grid points

K	Mode sequence					
	1	2	3	4	5	6
1	7.8968	16.8308	23.2632	28.1467	28.8140	35.8918
2	9.6278	16.8781	21.9549	30.5050	36.6110	44.5781
3	9.4954	16.0652	19.9348	25.5296	29.9872	36.5614
4	9.4899	15.9828	19.7824	24.7569	28.4890	34.5540
5	9.5009	15.9864	19.7415	24.6328	28.1985	34.1588
6	9.5012	15.9854	19.7324	24.5938	28.1445	34.0528
7	9.5025	15.9863	19.7334	24.5972	28.1349	34.0225
8	9.5025	15.9863	19.7334	24.5972	28.1349	34.0225
9	9.5027	15.9869	19.7338	24.5993	28.1342	34.0208
10	9.5028	15.9870	19.7337	24.6000	28.1341	34.0201
11	9.5028	15.9871	19.7338	24.6001	28.1341	34.0199
12	9.5028	15.9871	19.7338	24.6003	28.1339	34.0200
13	9.5028	15.9871	19.7338	24.6003	28.1340	34.0198
14	9.5028	15.9871	19.7338	24.6004	28.1339	34.0198
15	9.5028	15.9871	19.7338	24.6004	28.1339	34.0198
16	9.5028	15.9871	19.7338	24.6004	28.1339	34.0197

The MLS grid point size varies from 7×7 to 23×23 while the other parameters of the MLS-Ritz method are kept constants, i.e. $P = 3$, $k = 15$, $d = 0.5a$ and $N_g = 40$ for the two considered triangular plates (see Tables 14 and 15). The frequency parameters of the plates are well converged as the MLS grid point size reaches 15×15 and above. To ensure the accuracy of the results presented in this paper, we choose to use MLS grid point size 21×21 in all calculations for the right-angled isosceles triangular plates.

Table 17
Convergence of frequency parameters λ against the radius of support d for a simply supported right-angled isosceles triangular plate with $P = 3$, $k = 15$, $N_g = 40$ and 21×21 MLS grid points

d/a	Mode sequence					
	1	2	3	4	5	6
0.1	0.00E+00	1.69E+04	9.63E+04	1.41E+05	4.79E+05	1.48E+06
0.2	5.6841	10.8320	15.1712	19.1369	24.1942	28.1800
0.3	5.0002	10.0024	13.0017	17.0164	20.0164	25.0102
0.4	5.0000	10.0002	13.0001	17.0006	20.0010	25.0005
0.5	5.0000	10.0000	13.0002	17.0002	20.0004	25.0009
0.6	5.0000	10.0000	13.0001	17.0004	20.0008	25.0014
0.7	5.0000	10.0001	13.0001	17.0008	20.0026	25.0053
0.8	5.0000	10.0002	13.0007	17.0043	20.0047	25.0084

Table 18
Convergence of frequency parameters λ against the radius of support d for a clamped right-angled isosceles triangular plate with $P = 3$, $k = 15$, $N_g = 40$ and 21×21 MLS grid points

d/a	Mode sequence					
	1	2	3	4	5	6
0.1	4.08E+02	5.18E+02	6.23E+02	6.85E+02	7.42E+02	8.51E+02
0.2	9.4759	15.9653	19.6772	24.5378	28.0775	33.9297
0.3	9.5028	15.9869	19.7340	24.6004	28.1337	34.0206
0.4	9.5028	15.9871	19.7338	24.6003	28.1339	34.0199
0.5	9.5028	15.9871	19.7338	24.6004	28.1339	34.0198
0.6	9.5028	15.9871	19.7338	24.6004	28.1339	34.0198
0.7	9.5028	12.1274	15.9871	19.4608	19.7337	24.6004
0.8	9.5028	15.9870	17.3138	19.7334	24.6010	28.1358

Table 16 shows the variation of the frequency parameters of a clamped right-angled isosceles triangular plate versus the value of k in the MLS weight function. We observe that a wide range of k values can be used in the MLS-Ritz method to generate accurate vibration frequencies. In general, a larger value of k leads to better converged results. We choose to use $k = 15$ in this study for the vibration analysis of right-angled isosceles triangular plates.

The influence of the radius of support d of the MLS scheme on the frequency parameters of triangular plates is examined. Tables 17 and 18 present the variation of the frequency parameters of a simply supported and a clamped right-angled isosceles triangular plate against the radius of support d, respectively. We use $P = 3$, $k = 15$, $N_g = 40$ and 21×21 MLS grid points in this calculation. Similar to its square plate counterpart, a small radius of support d gives erroneous frequency parameters and a very large d value may lead to erroneous/missing modes as shown in the case for clamped triangular plate (see Table 18). Again, the optimal range of the radius of support d is observed to be between $0.4a$ and $0.6a$ in the considered triangular plate cases. We choose $d = 0.5a$ in the calculations.

Table 19
Comparison study of frequency parameters λ for right-angled isosceles triangular plates with $P = 3$, $k = 15$, $d = 0.5a$, $N_g = 40$ and 21×21 MLS grid points

Cases	Sources	Mode sequence					
		1	2	3	4	5	6
SSS	Present	5.0000	10.0000	13.0002	17.0002	20.0004	25.0009
	Ref. [32]	4.993					
	Ref. [13]	5.000	10.00	13.00	17.00		
	Ref. [33]	5.000	10.01	13.01	17.13	20.29	25.31
	Ref. [34]	4.999	9.970	13.03	17.43		
	Ref. [30]	5.001	9.998	13.00	17.00	20.09	25.12
CCC	Present	9.5028	15.9871	19.7338	24.6004	28.1339	34.0198
	Ref. [31]	9.48					
	Ref. [13]	9.510	15.98	19.74	24.60		
	Ref. [33]	9.5027	15.987	19.734	24.600	28.134	34.020
	Ref. [30]	9.502	15.99	19.74	24.62	28.17	34.19
CCF	Present	2.9477	6.4405	9.1042	11.7652	14.7511	19.1190
	Ref. [15]	2.927	6.379	9.085	11.66		
	Ref. [30]	2.948	6.439	9.104	11.77	14.76	19.13
FFC	Present	1.2812	3.6408	5.3627	8.5353	9.7153	13.3274
	Ref. [33]	1.282	3.641	5.363	8.552	9.750	13.36
	Ref. [30]	1.281	3.642	5.364	8.537	9.715	13.33
CSF	Present	1.8205	4.8582	7.4596	9.8285	12.4898	16.7246
	Ref. [33]	1.821	4.858	7.460	9.837	12.51	16.83
CCS	Present	7.4364	13.3319	16.7180	21.3304	24.5354	30.0250
	Ref. [14]	7.436	13.34	16.72	21.33		
	Ref. [34]	7.436	13.47	17.00	22.22		
	Ref. [30]	7.436	13.33	16.72	21.33	24.56	30.08

To confirm the correctness of the MLS-Ritz method for the vibration analysis of right-angled isosceles triangular plates, a comparison study is carried out against solutions obtained by other researchers [13–15,30–34] and the results for several selected triangular plates are presented in Table 19. Note that the study by Kitipornchai et al. [30] is based on the Mindlin shear deformable plate theory with small plate thickness to length ratio to simulate thin plates.

For a simply supported right-angled isosceles triangular plate (SSS plate), it is possible to obtain exact vibration solutions by using a simply supported square plate with appropriate modes of vibration [2]. For example, the exact frequency parameter of the first mode of the SSS triangular plate is 5 which is the same as the one for the second mode of the simply supported square plate. We observe that comparing with other numerical and analytical methods (see Table 19), the MLS-Ritz method generates very accurate frequency parameters for SSS right-angled isosceles triangular plate.

For a fully clamped right-angled isosceles triangular plate, the MLS-Ritz results are again in very close agreement with the ones by Gorman [13], Kim and Dickinson [33] and Kitipornchai et al. [30] As there are no known exact solutions available for this case, the convergence study given

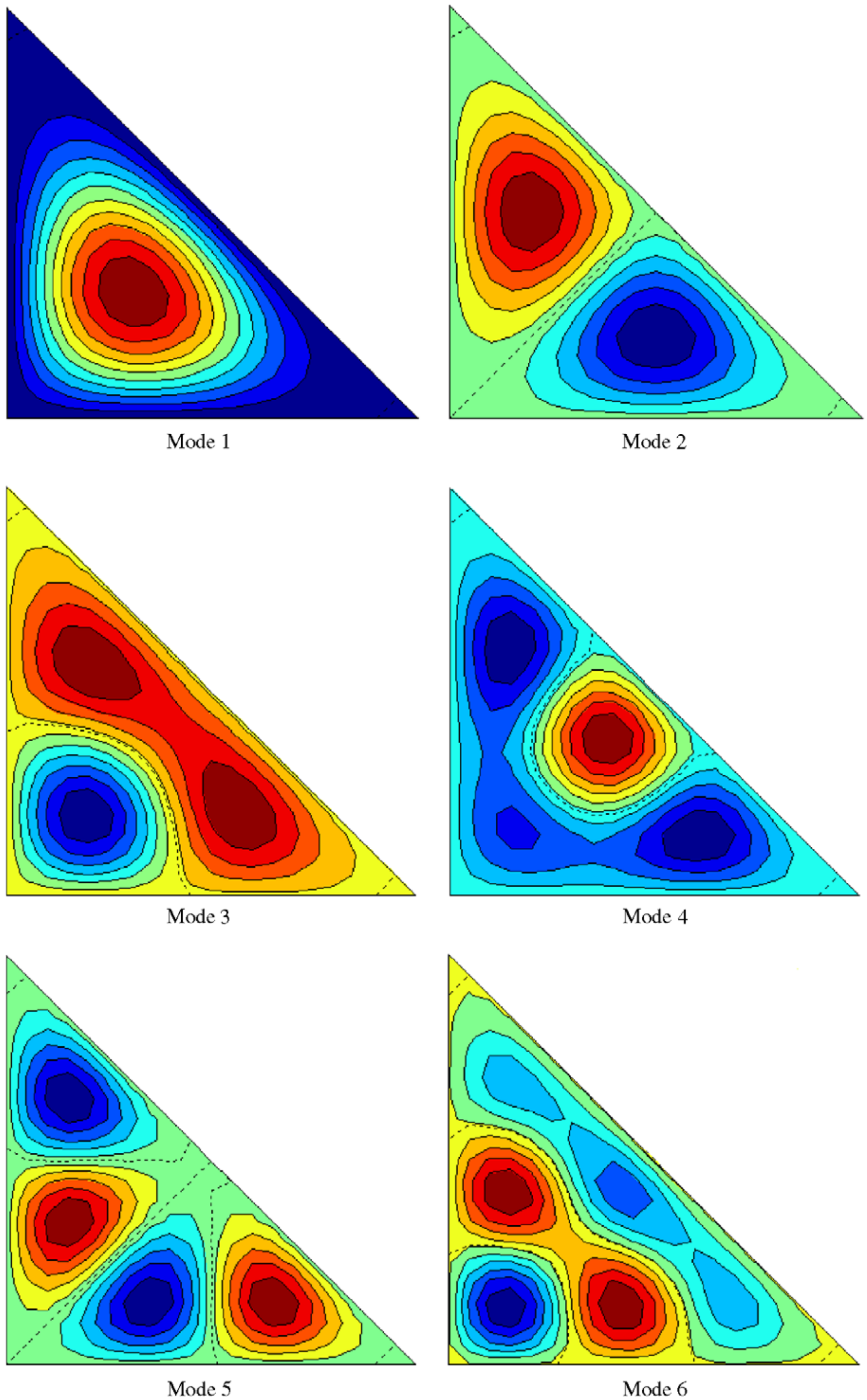

Fig. 6. Mode shapes for the first six modes of a simply supported right-angled isosceles triangular plate.

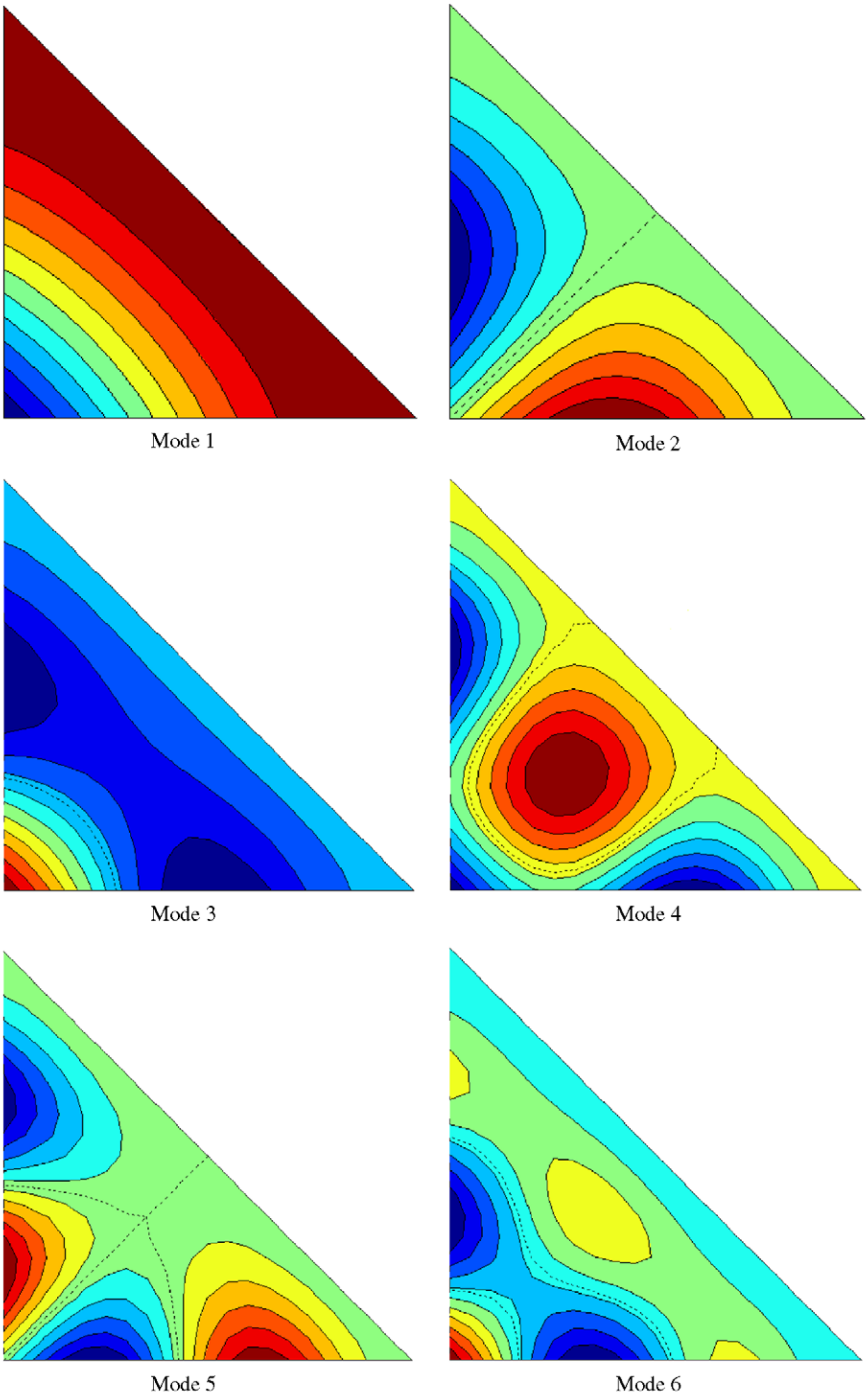

Fig. 7. Mode shapes for the first six modes of an FFC right-angled isosceles triangular plate.

in Table 15 together with the available solutions in the open literature is very useful to verify the accuracy of the current results.

Four other cases (CCF, FFC, CSF and CCS plates) are also compared with known solutions in the open literature (see Table 19). They all confirm the high accuracy of the MLS-Ritz method in the vibration analysis of right-angled isosceles triangular plates.

The first six vibration mode contour shapes of a simply supported right-angled isosceles triangular plate and an FFC right-angled isosceles triangular plate are presented in Figs. 6 and 7, respectively. We observe that the MLS-Ritz method can predict the correct vibration mode shapes for the considered cases. Note that the dotted contour lines in Figs. 6 and 7 represent the nodal lines of the vibration modes.

4. Conclusions

This paper has proposed a novel numerical method, the MLS-Ritz method, for the vibration analysis of thin plates. The MLS technique has been employed to establish the Ritz trial function for the transverse displacement of a plate. A point substitution technique has been proposed to enforce the geometric boundary conditions of the plate. Convergence studies have been carried out to determine the size of the MLS grid points, the number of Gaussian points, the degree of 2-D polynomial basis function and the MLS radius of support that are required to produce accurate MLS-Ritz vibration results. Comparison studies have proven that the proposed method is highly accurate for predicting the vibration frequencies of plates. Further studies on the versatility and applicability of the method are being carried out and the research findings will be reported in future publications.

References

[1] E.F.F. Chladni, Entdeckungen uber die Theorie des Klanges, Leipzig (1787).
[2] A.W. Leissa, Vibration of Plates, US Government Printing Office, NASA SP-160 (1969), reprinted by the Acoustical Society of America (1993).
[3] A.W. Leissa, The free vibration of rectangular plates, *Journal of Sound and Vibration* 31 (1973) 257–293.
[4] R.B. Bhat, Flexural vibration of polygonal plates using characteristics orthogonal polynomials in two variables, *Journal of Sound and Vibration* 114 (1987) 65–71.
[5] K.M. Liew, C.M. Wang, Y. Xiang, S. Kitipornchai, *Vibration of Mindlin Plates—Programming the p-Version Ritz Method*, Elsevier Science, Oxford, 1998.
[6] Y. Xiang, C.M. Wang, Exact buckling and vibration solutions for stepped rectangular plates, *Journal of Sound and Vibration* 250 (2002) 503–517.
[7] A.W. Leissa, Recent research in plate vibrations: classical theory, *Shock and Vibration Digest* 9 (10) (1977) 13–24.
[8] A.W. Leissa, Recent research in plate vibrations: complicating effects, *Shock and Vibration Digest* 9 (11) (1977) 21–35.
[9] A.W. Leissa, Plate vibration research: 1976–1980: classical theory, *Shock and Vibration Digest* 13 (9) (1981) 11–22.
[10] A.W. Leissa, Plate vibration research: 1976–1980: complicating effects, *Shock and Vibration Digest* 13 (10) (1981) 19–36.
[11] A.W. Leissa, Recent research in plate vibrations: 1981–1985: part I. Classical theory,, *Shock and Vibration Digest* 19 (2) (1987) 11–18.

[12] A.W. Leissa, Recent research in plate vibrations: 1981–1985: part I. Complicating effects,, *Shock and Vibration Digest* 19 (3) (1987) 10–24.
[13] D.J. Gorman, A highly accurate analytical solution for free vibration analysis of simply supported right triangular plates, *Journal of Sound and Vibration* 89 (1983) 107–118.
[14] D.J. Gorman, Free vibration analysis of right triangular plates with combinations of clamped-simply supported boundary conditions, *Journal of Sound and Vibration* 106 (1986) 419–431.
[15] D.J. Gorman, Accurate analytical solution for free vibration of the simply supported triangular plate, *AIAA Journal* 27 (1989) 647–651.
[16] A.A. Khdeir, Free vibration and buckling of symmetric cross-ply laminated plates by an exact method, *Journal of Sound and Vibration* 126 (1988) 447–461.
[17] W.C. Chen, W.H. Liu, Deflections and free vibrations of laminated plates-Levy-type solutions, *International Journal of Mechanical Sciences* 32 (1990) 779–793.
[18] U.S. Gupta, S.K. Jain, D. Jain, Method of collocation by derivatives in the study of axisymmetric vibration of circular plates, *Computers and Structures* 57 (1995) 841–845.
[19] M. Mukhopadhyay, Vibration and stability analysis of stiffened plates by semi-analytic finite difference method, part I: consideration of bending displacements only, *Journal of Sound and Vibration* 130 (1989) 27–39.
[20] G. Karami, P. Malekzadeh, Application of a new differential quadrature methodology for free vibration analysis of plates, *International Journal for Numerical Methods in Engineering* 56 (2003) 847–868.
[21] T. Belytschko, Y. Krongauz, D. Organ, M. Fleming, P. Krysl, Meshless methods: an overview and recent developments, *Computer Methods in Applied Mechanics and Engineering* 139 (1996) 3–47.
[22] Y.K. Cheung, *Finite Strip Method in Structural Mechanics*, Pergamon Press, Oxford, 1976.
[23] P.R. Heyliger, J.N. Reddy, A higher-order beam finite-element for bending and vibration problems, *Journal of Sound and Vibration* 126 (1988) 309–326.
[24] R. Bellman, B.G. Kashef, J. Casti, Differential quadrature: a technique for the rapid solution of nonlinear partial differential equations, *Journal of Computational Physics* 10 (1972) 40–52.
[25] C. Shu, C.M. Wang, Treatment of mixed and nonuniform boundary conditions in GDQ vibration analysis of rectangular plates, *Engineering Structures* 21 (1999) 125–134.
[26] G.W. Wei, Y.B. Zhao, Y. Xiang, Discrete singular convolution and its application to the analysis of plates with internal supports. Part 1: theory and algorithm,, *International Journal for Numerical Methods in Engineering* 55 (2002) 913–946.
[27] Y.B. Zhao, G.W. Wei, Y. Xiang, Discrete singular convolution for the prediction of high frequency vibration of plates, *International Journal of Solids and Structures* 39 (2002) 65–88.
[28] K.M. Liew, Y.Q. Huang, Bending and buckling of thick symmetric rectangular laminates using the moving least-squares differential quadrature method, *International Journal of Mechanical Sciences* 45 (2003) 95–114.
[29] L. Zhou, J.G. Zhu, Application of MLSDQ method for analysis of electromagnetic fields, *The Proceedings of the 2003 Australasian Universities Power Engineering Conference (AUPEC 2003)*, Paper No. 161, Christchurch, New Zealand, 2003.
[30] S. Kitipornchai, K.M. Liew, Y. Xiang, C.M. Wang, Free vibration of isosceles triangular Mindlin plates, *International Journal of Mechanical Sciences* 35 (1993) 89–102.
[31] T. Ota, M. Hamada, T. Tarumoto, 1961, *Fundamental frequency of an isosceles triangular plate, Bulletin of Japan Society of Mechanical Engineers (JSME)* 4 (1961) 478–481.
[32] H.D. Conway, K.A. Farnham, The free flexural vibrations of triangular rhombic and parallelogram plates and some analogics, *International Journal of Mechanical Sciences* 7 (1965) 811–816.
[33] C.S. Kim, S.M. Dickinson, The free flexural vibration of right triangular isotropic and orthotropic plates, *Journal of Sound and Vibration* 141 (1990) 291–311.
[34] K.Y. Lam, K.M. Liew, S.T. Chow, Free vibration analysis of isotropic and orthotropic triangular plates, *International Journal of Mechanical Sciences* 32 (1990) 455–464.